

## Systematic study of the response of single crystal diamond neutron detectors at high temperature

M. Angelone,<sup>a</sup> R. Pilotti,<sup>b</sup> F. Sarto,<sup>a</sup> M. Pillon,<sup>a</sup> S. Lecci,<sup>a</sup> S. Loreti,<sup>a</sup> G. Pagano,<sup>a</sup> S. Cesaroni,<sup>b,1</sup> C. Verona,<sup>b</sup> M. Marinelli,<sup>b</sup> G. Prestopino<sup>b</sup> and G. Verona-Rinati<sup>b</sup>

<sup>a</sup>Dipartimento Fusione e Tecnologie per la Sicurezza Nucleare, ENEA C.R. Frascati, via E. Fermi, 45, Frascati 00044, Italy

<sup>b</sup>Dipartimento di Ingegneria Industriale, Università degli Studi di Roma "Tor Vergata", via del Politecnico, 1, Roma 00100, Italy

E-mail: [silvia.cesaroni@uniroma2.it](mailto:silvia.cesaroni@uniroma2.it)

**ABSTRACT:** For many years artificial diamond detectors have been studied for application in high temperature environments. An open question is whether the performance of such detectors is influenced by the electrical contacts. In the attempt to better understand this point, a systematic study of electrical contacts deposited with different techniques and materials on top of commercial artificial single crystal diamond (SCD) films was performed. In this paper we report on the results obtained using three types of electric contacts produced both using metal and not metal layers: *a*) double Schottky, *b*) double ohmic; *c*) Schottky-ohmic contacts. The detectors were studied under 14 MeV neutron irradiation, and were operated in pulse mode. The pulse height spectra (PHS) produced by the 14 MeV neutrons were recorded as a function of temperature and the detector behaviour was studied by analysing the variation of the peak produced in the PHS by the  $^{12}\text{C}(n, \alpha)^9\text{Be}$  reaction induced by 14 MeV neutrons in carbon.

The maximum operational temperature limit of the tested detectors was found to be around 230°C and it resulted to be slightly dependent, within  $\pm 10^\circ\text{C}$ , upon the type of the electrical contact. It turned out that, together with the type of the electrical contact, other parameters such as the intrinsic diamond properties and the film thickness have to be considered to understand the response of the detector at high temperature.

**KEYWORDS:** Diamond Detectors; Neutron detectors (cold, thermal, fast neutrons); Solid state detectors; Instrumentation for neutron sources

<sup>1</sup>Corresponding author.

---

## Contents

<b>1</b>	<b>Introduction</b>	<b>1</b>
<b>2</b>	<b>Diamond detectors and electrical contacts</b>	<b>3</b>
2.1	Detector fabrication	4
2.2	Electrical contacts	5
2.3	Deposition of electrical contacts	5
<b>3</b>	<b>Neutron detection with diamond detectors</b>	<b>6</b>
<b>4</b>	<b>Experimental procedure</b>	<b>7</b>
<b>5</b>	<b>Results</b>	<b>8</b>
5.1	Detectors with Schottky-Schottky contacts	8
5.1.1	Cr-Cr contacts on 500 $\mu\text{m}$ thick diamond	8
5.1.2	Cr-Cr contacts on 100 $\mu\text{m}$ thick diamond	10
5.1.3	Tungsten contacts on 500 $\mu\text{m}$ thick diamond plate	11
5.2	Schottky-ohmic configuration	12
5.2.1	Detector fabrication and characterization	13
5.2.2	Results for the 100 $\mu\text{m}$ thick layered detector under neutron irradiation	15
5.2.3	Layered detector 500 $\mu\text{m}$ thick	16
<b>6</b>	<b>Discussion</b>	<b>19</b>
<b>7</b>	<b>Conclusions</b>	<b>20</b>

---

## 1 Introduction

Diamond detectors operated at high temperature have been studied for many years as candidate neutron monitors for nuclear fusion reactors. The possibility of using diamond is related to the outstanding properties of this material [1, 2]. Indeed, diamond shows the highest thermal conductivity ( $22 \text{ W cm}^{-1} \text{ K}^{-1}$ ), high electrical resistance and high carrier mobility (the highest for holes) at room temperature. These detectors are proposed for plasma diagnostics as well as for monitoring fundamental nuclear parameters of the tokamaks, e.g. the on-line tritium production [3]–[6]. Let mention that tritium is the fuel for tokamaks operating with Deuterium-Tritium plasma. However, for operation in fusion machines, the detectors have to withstand very harsh working conditions characterized by high temperature (up to  $550^\circ\text{C}$ ), intense neutron and gamma fluxes ( $> 10^{14} \text{ cm}^{-2} \text{ s}^{-1}$ ), intense magnetic field (up to 5 T) and electrical-magnetic (EM) noises. It ought to be stressed that presently there is not instrumentation ready to withstand the harsh working condition of fusion reactors and research is ongoing to develop suitable detectors to operate in fusion

machine environments [7]. A discussion about the requirements and constraints to be fulfilled by these nuclear detectors is reported in [8].

The present work is the follow-up of preliminary studies on commercial diamond detectors designed for room temperature operation, operated at increasing temperatures [9] upon irradiation with alphas and 14 MeV neutrons, with the aim of studying their response and performance versus temperature. These studies concluded that: *a*) the operational performance first slowly degraded with temperature and then was lost above about 160° C; this operational limit was mainly ascribed to the lay-out of the detector and to materials (except for the diamond film itself) used for its fabrication; *b*) as a consequence of the previous point, to operate at higher temperature (HT) (i.e., above 150° C) the diamond detectors must be fabricated by using dedicated materials and technologies able to withstand HTs.

Diamond detectors able to operate up to 230–240° C, realized without dedicated materials, were reported [10]. However these detectors were operated in vacuum, and realized with a design far away from that needed for operating e.g. in the tritium breeding module (TBM) of ITER where penetration of 5 mm are available for hosting the detectors and severe constraints and integration rules are to be fulfilled.

In a previous paper, some of the present authors reported on a prototype detector, fabricated according to previous point *b*), which was realized at ENEA Frascati using a 500 μm thick single crystal diamond (SCD) film, and Ag electrical contacts. The latter were post-deposition annealed at 600° C in void. This detector was able to operate in spectrometric mode with high energy resolution (FWHM ~ 4%) and excellent stability, up to about 230–235° C [11], above which the performance degraded. The detector lay-out used in ref. [11] and specifically designed for high temperature application (up to 400° C), was also used in the present work and it is briefly presented in section 2.1. An issue with the Ag contacts was the degradation of the detector performance with the operational time as well as the fact that the limit of 240° C is still low for some applications of diamond detectors in tokamaks.

As a consequence of the previous study an open question is still whether the performance of SCD detectors operating at HT (referred to as SCDDs-HT in the following) is influenced, and how much, by the type and the deposition process of the electrical contacts. In the attempt to improve the performance of the SCDDs-HT and to understand the causes limiting their operation, a systematic study of different types of electrical contacts deposited with different materials and methods on top of commercial artificial SCD films was performed.

It is well known that in a semiconductor two types of metal-semiconductor electrical contacts can be usually formed, the so-called ohmic and Schottky-type contacts, which are characterized by different I-V characteristics and electrical resistance. The ohmic and Schottky contacts can be obtained using different deposition processes and materials; this will shortly be addressed in section 2.

The aim of this paper is to present the results of the systematic work discussed above, so to complement the work reported in [11]. Commercial SCD films, of the so called *electronic grade quality*, produced by Element-6 company [12], were used. The detectors, fabricated with the different types of electrical contacts, were characterized in term of I-V characteristics versus biasing voltage (HV) and temperature, and eventually tested analysing the PHS spectra recorded at increasing temperatures under 14 MeV neutron irradiation at the ENEA-Frascati neutron generator

(FNG) [13]. The study was carried out performing measurements in pulse mode (i.e., spectroscopic mode). It is worth to point out that, owing to the huge quantity of data obtained in our study due to the attempt to gather as much as possible statistical information to prove the experimental reproducibility, hereafter we report only a selection of the available results.

The paper first recalls the main properties and problems of diamonds electrical contacts by presenting the different types of diamond detectors realized for this study (section 2). In section 3 the principle of diamond-neutron interaction are recalled. The experimental procedure is presented in section 4, while the results are reported in section 5. A discussion of the results is addressed in section 6, while the conclusions are reported in section 7.

## 2 Diamond detectors and electrical contacts

The high specific resistivity of diamond ( $>10^{13} \Omega \text{ cm}$ ), which makes the diamond detector a “solid state ionization chamber”, allows, in principle, for a very simple construction of the detector. In its simplest form, a diamond detector can be made by depositing two metal contacts on the opposite surfaces of the diamond film, while a biasing high voltage (HV) is applied between the two electrodes; this is the so-called *back-to-back* configuration. However, different configurations and types of detectors can be produced depending upon the used materials (e.g. metal type) and the technique employed to deposit the electric contacts onto the diamond film surfaces. The questions are whether and how much the type of electrical contact affects the response of the diamond detector when operated at HT, and which type of electrical contact is better suited for operation at high temperature. As a matter of fact, in the literature a systematic study of the response of diamond detectors made with commercial diamond films and equipped with electrical contacts realized with different materials and deposition techniques, is missing.

Depending upon the fabrication procedure, the metal-diamond junction forms either *Schottky* or *ohmic* contacts. The former is usually obtained when a metal layer is just deposited (either by sputtering or thermal evaporation technique) on a diamond surface. In this case a rectifying junction is formed at the metal-diamond interface (the physical dimensions along thickness direction are of a few atomic layers), characterized by a typical electrical potential (namely, the Schottky barrier) due to the difference in between the *work functions* of metal and diamond. The magnitude of the barrier depends upon the type of metal, and typically ranges from 0.5 to 1 eV. For a detailed analysis of the Schottky barrier properties see [14–16]. As for the ohmic contacts, different techniques can be used for their production, as discussed in the following (section 2.3). The ohmic contacts are characterized for an almost linear dependence between the current flowing through the detector contacts (electrodes) and the voltage applied to the two electrodes as well as low electrical resistance. Last, but not least, it is recalled that an ohmic contact must have low resistivity, good adhesion, high thermal stability, high corrosion resistance, bondable top-layer and suitability for micro-patterning [17]. Indeed, all these properties, but the first, apply to Schottky contacts too.

Previous studies [17, 18] pointed out important issues related to electrical contacts that need to be solved to allow a reliable operation of the SCDD-HT. Among them, let mention:

- a) *Metallization*. Conventional or inadequate contact fabrication may result in poor mechanical adhesion, polarization effects and unrepeatable results.

- b) *Mechanical Adhesion*. That is the mechanical adhesion of the metal chosen as electrode on the diamond surface. To note that a flat smooth surface, like that of diamond, presents few adhesion points. When a metal is thermally evaporated on diamond it may not adhere and it could peel-off (after a period of time) with the consequent deterioration of the electrical signal and therefore a decrease in the device lifetime. Mechanical adhesion is a function of the diamond/contact interface. The peeling was observed in a previous study, after short operation time at HT [9].
- c) *Polarization Effects*. Polarization phenomena occur when electric currents pass through diamond if the electrical contact is not able to extract and inject carriers fast enough. In this case, the neutrality of the crystal after the passage of ionizing nuclear radiation is not restored in the time interval between two consecutive events, and the detector loses its stability. As a result, charge accumulation occurs within the crystal and immobile carriers establish an electric field which acts in a direction opposite to the field produced by the external bias. The minimisation of polarization effects requires optimal injecting contacts.

This work was performed in the attempt to better understand some of the questions above.

## 2.1 Detector fabrication

The diamond films used in this work were monocrystalline SCD plates ( $4.3 \times 4.3 \text{ mm}^2$  surface) with variable thickness of  $100 \mu\text{m}$ ,  $300 \mu\text{m}$  and  $500 \mu\text{m}$ , purchased by Element-6 company [12]. All the used diamond plates were of the so-called *electronics purity grade* that means, according to the information provided by the manufacturer, that the diamond films are characterized by an amount of nitrogen and boron impurities lower than 5 ppb [12]. Before deposition of electrical contacts and regardless of the type of metal, all the diamond plates were annealed in vacuum at  $500^\circ\text{C}$  for 1 hour.

A diamond detector lay-out which makes use of mineral cable (MI) and metal-oxide connectors (MOC) was designed at ENEA to operate at HT prior to the present study [11]. The technical characteristics of this prototype detector allow its use up to  $400^\circ\text{C}$ . MI, made with stainless steel central conductor (1 mm diameter) and  $\text{Al}_2\text{O}_3$  insulator, is used since it is able to withstand temperatures up to  $800^\circ\text{C}$  as well as high neutron fluence ( $>10^{20} \text{ n/cm}^2$ ) while the used MOC can operate up to  $400^\circ\text{C}$ . The latter component can be eliminated by directly connecting the central conductor of the MI cable to the diamond film. A picture of this detector is shown in figure 1. The diamond plate is directly connected to the central wire of the MI and it is grounded by the L-shaped copper element behind it, which is connected to the stainless steel chassis by a screw and a spring. The electrical contacts are realized by mechanical constrains and pressure, not other means (e.g. glue) are used. More details can be found in [11].

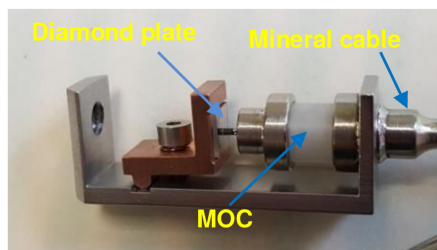


**Figure 1.** Picture of the diamond detector developed for this work. The main elements are also indicated.

## 2.2 Electrical contacts

Different metals (Cr, WC, Pt/Ti, Boron-Cr) and deposition techniques (sputtering or evaporation), as well as possible post deposition thermal treatment (annealing or not annealing in oven) were used in the attempt to produce both ohmic and Schottky type electrical contacts. The goal was to find out suitable solutions for the electrical contact fabrication process which allowed for a reliable, reproducible, stable and long lasting use of the fabricated SCDD-HT. Another goal was to increase the operational temperature limit of  $\sim 230^\circ\text{C}$  already reported in [10, 11]. Here after a short description of the different techniques employed for the deposition of the used electrical contacts is reported.

## 2.3 Deposition of electrical contacts

- a) *Deposition of rectifying metal contacts (Schottky diode).* It is known that a metal-diamond structure normally forms a Schottky diode, that is a rectifying contact featuring a typical electrical potential (Schottky barrier,  $\Phi_B$ ) [19]. The magnitude of  $\Phi_B$  is the difference between the *work functions* of the metal and carbon respectively, and therefore it depends upon the used metal. Table 1 lists the  $\Phi_B$  data for the metals used in this work. As a result, when a metal is deposited on both the surfaces of the diamond plate a *double Schottky-diode* is obtained. The metal contacts (usually  $3 \times 3 \text{ mm}^2$  surface or 3 mm in diameter) were deposited at ENEA by sputtering technique or at Rome “Tor Vergata” University by evaporation technique, with the goal to look at possible differences in the Schottky contact performance attributable to the deposition method.
- b) All the deposited metal films were typically 100 nm thick, however for the case of the double layered contact Pt/Ti, the Ti film, deposited on top of the 100 nm thick Pt film in order to avoid oxidation, was 30 nm thick.

**Table 1.** Work functions for diamond and the metals used as contact for the detectors realized for the present work. Column three reports the type of electrical contacts: *a)* Schottky stands for not annealed, *b)* ohmic means metal annealed (for some metals both options were studied). Column four reports the used annealing procedure in void. (*Note:* Data selected from the articles [18, 19].)

Material	Work function (eV)	Type of contact	Annealing
<b>Ti</b>	4.3	<i>Schottky</i>	<i>No</i>
<b>Cr</b>	4.5	<i>Schottky</i>	<i>600°, 1 h</i>
<b>Au</b>	5.1	<i>Schottky</i>	<i>No</i>
<b>Pt</b>	5.7	<i>Schottky</i>	<i>No</i>
<b>Cu</b>	4.65	<i>Schottky and ohmic</i>	<i>600°, 1 h</i>
<b>Ag</b>	4.29	<i>Schottky and ohmic</i>	<i>600°, 1 h</i>
<b>W</b>	4.55	<i>ohmic</i>	<i>600°, 1 h</i>
<b>Diamond</b>	4.8 ÷ 5.8		

- c) *Deposition of ohmic contacts.* To produce ohmic electrical contacts some of the metal contacts deposited as discussed in point *a)* above were post deposition annealed in oven, in vacuum condition, for 1 h at  $600^\circ\text{C}$ . This was done for Ag, Cu and W metal contacts.

d) Detectors with the *Schottky-ohmic configuration* were also produced. The ohmic contact was realized with a different technique and deposited only onto one of the two diamond plate surfaces, while on the other side a Schottky contact, realized as discussed in a), was deposited by evaporation technique using Chromium. The ohmic contact, in turn, was produced by depositing directly on top of the diamond plate, an heavily boron doped ( $> 10^{20} \text{ cm}^{-3}$ ) diamond layer (1–2  $\mu\text{m}$  thick), by means of a microwave-assisted plasma-enhanced chemical vapour deposition (MW-PECVD) technique (see ref. [20] for details). In the following this contact will be referred to as *boron-contact*. To note that Schottky-ohmic diamond detectors are extensively used for UV and X-ray measurements as well as in X-ray dosimetry applications [21, 22]. Moreover, at the best of the authors' knowledge, the *boron-contact* was studied at high temperature for the first time in the present work; this is why it will be more extensively discussed in section 5.2. The three different diamond detector configurations described above are shown in figure 2.

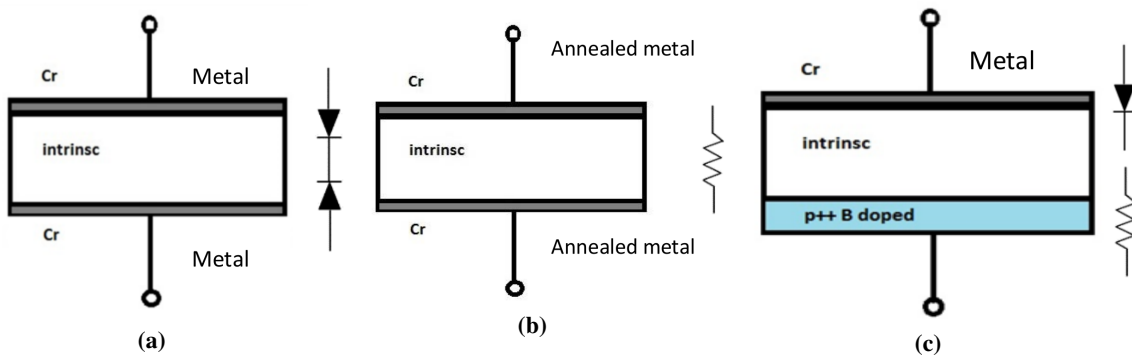


**Figure 2.** Schematic representation of the three diamond detector configurations used in this work: a) Schottky-Schottky; b) Ohmic-ohmic; c) Schottky-ohmic. The respective equivalent circuit models are reported next to each figure.

### 3 Neutron detection with diamond detectors

Natural Carbon (99%  $^{12}\text{C}$  and 1%  $^{13}\text{C}$ ) reacts with fast neutrons via many reactions, a detailed list can be found in table 2 of reference [23]. In the present paper we focus on the  $^{12}\text{C}(n, \alpha)^9\text{Be}$  reaction which has a neutron energy threshold of about 5.7 MeV and produces a sharp and well isolated peak in the pulse height spectrum. This reaction is used for measuring the 14 MeV neutron emission in tokamaks [24, 25]. Figure 3a shows a typical pulse height spectrum (PHS) recorded at room temperature under 14 MeV neutron irradiation. For the sake of this paper we will be interested in the behaviour, as a function of temperature, of the  $^{12}\text{C}(n, \alpha)^9\text{Be}$  peak, whose position (centroid), energy resolution (FWHM) and area will be considered (figure 3b). The analysis of the peak features at different temperatures was performed by comparing the three parameters mentioned above to those measured at room temperature, keeping constant the working parameters of the detectors (HV and electronics). The mentioned parameters were derived by peak fitting procedure.

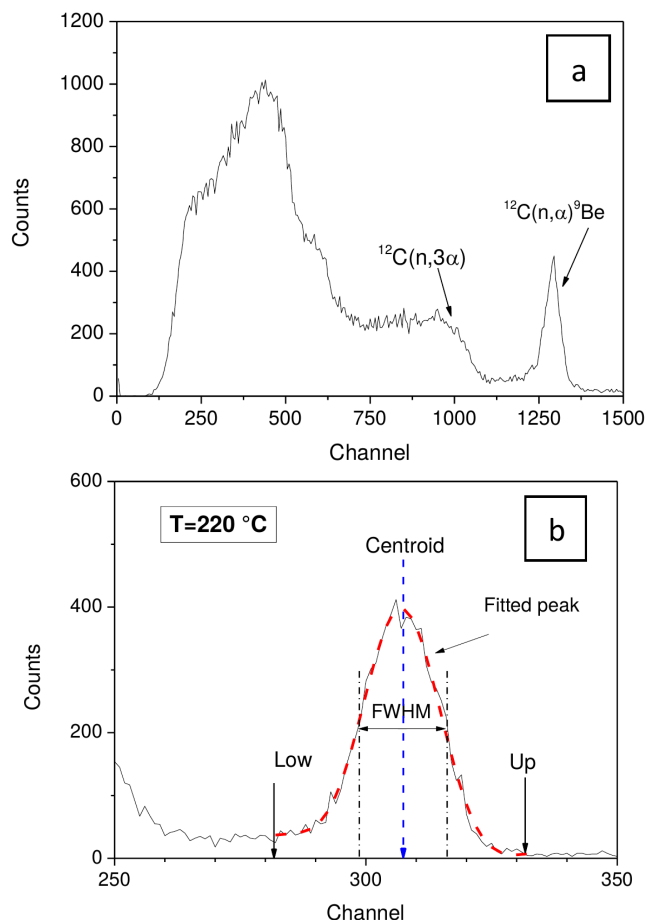


**Figure 3.** *a)* Typical PHS recorded by a diamond detector irradiated with 14 MeV neutrons at room temperature. The main neutron-C interactions are evidenced; *b)* Example of the  $^{12}\text{C}(n, \alpha)^9\text{Be}$  peak analysis and its main parameters (220°C temperature).

#### 4 Experimental procedure

The experimental procedure adopted to study the detector response at HT was the same for all the evaluated detectors, regardless of the type of electrical contacts. Each diamond detector was first studied by measuring the current-voltage (I-V) characteristics. After that, the detector was irradiated with 14 MeV neutrons at the Frascati neutron generator (FNG) [13] at increasing temperature, up to the operational limit. Then the detector was cooled down and the measurements were repeated by cycling the same procedure two or more times to study the reproducibility.

For the measurement at HT a cylindrical heater, made by a double solenoid to null the magnetic field produced by the two opposite currents, was used. The heater can operate under stable temperature up to 450°C. Once the requested working temperature ( $T_0$ ) was reached, it was kept constant ( $T = T_0 \pm 1^\circ\text{C}$ ) for the whole duration of the measurements thanks to a dedicated software. The temperature was measured by means of a K-type thermocouple (range up to 1000°C). All the measurements were performed in air.

The used electronics was always the same and consisted of a picoammeter Keithley 6517 with internal high voltage ( $\pm 500$  V max.) for I-V measurement, CAEN N1470 HV module, charge preamplifier (ORTEC 142A), pulse amplifier (ORTEC 572) and multichannel analyser (MCA) for PHS acquisition and multi-channel scaler (MCS) for time dependent detector response recording. In some cases a fast electronics, making use of a fast digitizer (CAEN DT 5724 PHA digitizer) was used too. The digitizer allowed to operate in *list mode*, so to record the pulse amplitudes as a function of the irradiation time (bi-dimensional matrix). This allowed to extract the PHS at the desired time and temperature.

The measurements consisted in the simultaneous acquisition of the PHS (see figure 3a) and MCS spectra at various temperatures, starting from room temperature. In some cases the same diamond film was re-used two or even more times for fabricating a new detector with different electrical contacts. To this end, the old metallic contacts were removed and the diamond surfaces were cleaned by means of a bath in acid solution followed by rinsing in deionised water; the diamond plate was then annealed in oven at  $500^\circ\text{C}$  for 1 h. In our experience the re-use of the diamond film did not affect the performance of the new fabricated detector provided the cleaning procedure was carefully performed.

## 5 Results

In the following we report at first the results for the diamond detectors equipped with two metal contacts. Results for both as deposited (double Schottky) and post-deposition annealed contacts (double-ohmic) are presented. The results for the Ag and Pt/Ti electrical contacts were already reported in [11] and are no longer discussed here.

### 5.1 Detectors with Schottky-Schottky contacts

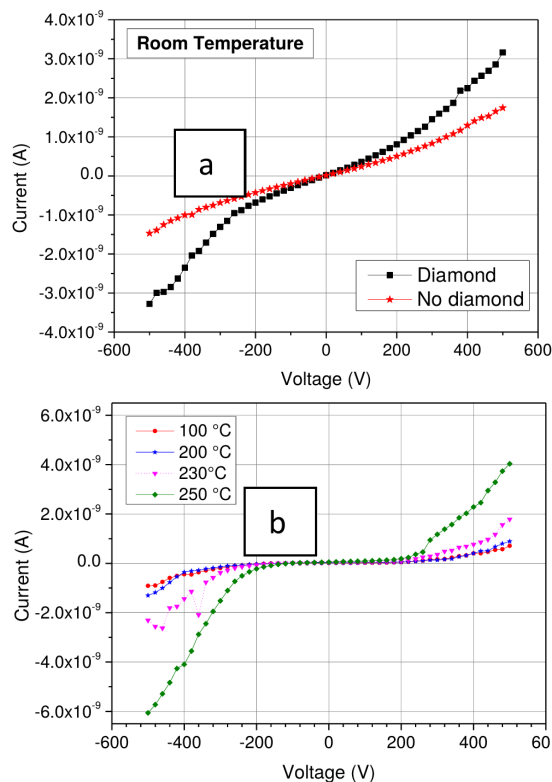
#### 5.1.1 Cr-Cr contacts on $500\ \mu\text{m}$ thick diamond

A  $500\ \mu\text{m}$  thick diamond plate was used. Two chromium metal contacts, 3 mm diameter and 100 nm thick, were deposited by thermal evaporation technique on both surfaces of the diamond plate. The I-V characteristics were measured as reported in section 4. The measurements were performed both at increasing temperature but also removing the diamond film from the detector, so to measure the effect of the mineral cable (see figure 4) on the measured current.

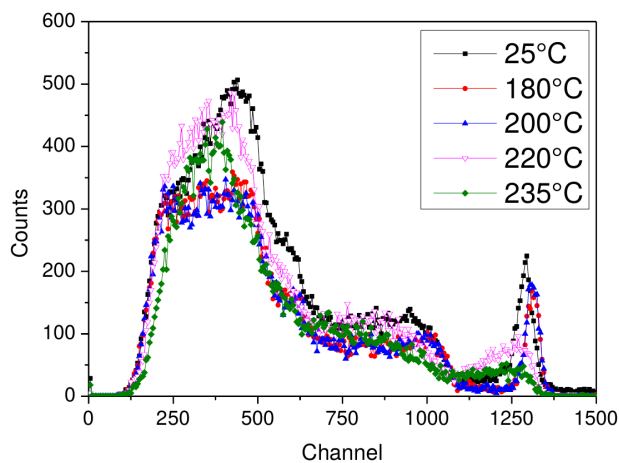
The detector was thus irradiated with 14 MeV neutrons at FNG. The detector was operated with  $0.7\ \text{V}/\mu\text{m}$  bias and the electronics chain was as already discussed in section 3. The data were collected by CAEN DT5724 PHA digitizer.

Figure 5 shows the PHS recorded as a function of temperature while figure 6 displays both the energy resolution (FWHM) and the position of the centroid of the  $^{12}\text{C}(n, \alpha)^9\text{Be}$  peak as a function of temperature.

Figures 5 and 6 clearly indicate that the detection properties are barely influenced by the temperature up to  $\sim 200^\circ\text{C}$ . Up to this temperature the  $^{12}\text{C}(n, \alpha)^9\text{Be}$  peak is well distinguishable from the background, but for  $T > 200^\circ\text{C}$  the degradation of the peak shape becomes evident; the peak centroid is shifted to lower channels and there is a clear worsening of the energy resolution. This last phenomenon was already observed and it is consistent with other studies [10, 11].



**Figure 4.** *a)* Leakage current measured at room temperature with and without the diamond film connected to the detector chassis, the difference due to the presence of the diamond film is evident; *b)* Leakage current versus bias voltage recorded at increasing temperature for the detector with two Cr metal contacts. To note the steep increase for  $T > 200^{\circ}\text{C}$ .



**Figure 5.** 14.1 MeV PHS recorded as function of temperature; Cr-Cr configuration.

In figure 7 the time dependent behaviour of the diamond detector as recorded by the digitizer in the temperature range 180–220 °C is shown. The vertical axis of figure 7 reports the pulse amplitudes (pulse height) in unit of MeV. The horizontal axis reports the measuring time. The temperature vs. time is also reported (orange curve, right axis). To note that the digitizer allows to clearly separate

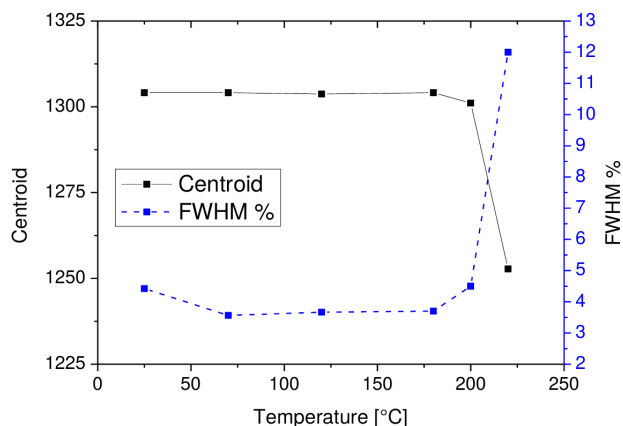


**Figure 6.** Energy resolution related to the  $^{12}\text{C}(n, \alpha)^9\text{Be}$  peak as function of temperature (black line, right axis) and  $^{12}\text{C}(n, \alpha)^9\text{Be}$  peak centroid as function of the temperature (blue line, left axis); Cr-Cr configuration.

the  $^{12}\text{C}(n, \alpha)^9\text{Be}$  peak of interest (thick light blue line at about 8,3 MeV) from the other reactions contributing to the PHS spectrum (see figure 7). When the temperature approaches  $220^\circ\text{C}$  the events at about 8.3 meV tend to drop toward lower values. By further increasing temperature the diamond detector paralysed as well evidenced in figure 7. Indeed for  $T > 210^\circ\text{C}$  (see the right side of the figure) the separation between the sharp line due to the  $^{12}\text{C}(n, \alpha)^9\text{Be}$  peak tends to bend and overlap to the background. It must be remarked that this phenomenon results reversible. Once the temperature decreased below  $210^\circ\text{C}$  the detection performance of the detector were re-established. Even repeating (by cycling) this procedure the detector always restored the detection capabilities when  $T < 200^\circ\text{C}$ .

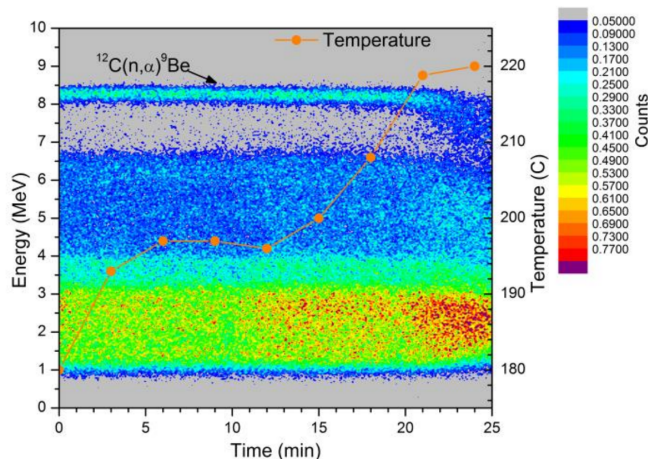


**Figure 7.** Pulse height (expressed in MeV) temporal distribution as function of the temperature; Cr-Cr configuration.

### 5.1.2 Cr-Cr contacts on $100\ \mu\text{m}$ thick diamond

A second detector was realized with Cr metal contacts by using a  $100\ \mu\text{m}$  thick diamond film. The deposition procedure and the experimental techniques were the same as discussed above for the case of the  $500\ \mu\text{m}$  thick Cr-Cr detector. The results are summarized in figures 8 and 9.

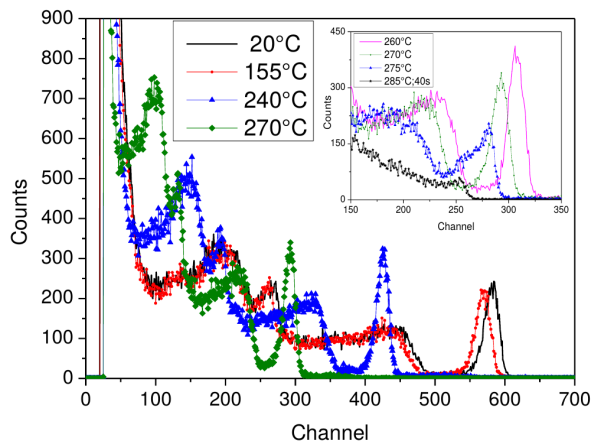


**Figure 8.** PHS spectra recorded for the 100 mm thick Cr-Cr detector.

Now the detector shows well-shaped and resolved peaks due to the  $^{12}\text{C}(n, \alpha)^9\text{Be}$  reaction up to about 270°C, however, as soon as the temperature increases further a clear loss of the detector performances is observed. For  $T > 285^\circ\text{C}$  the detection performance was almost completely lost (see inset in figure 8). Again, cooling down the detector below 200°C the detection capabilities were re-established.

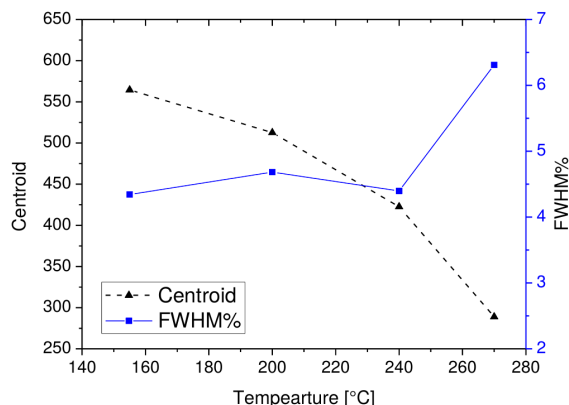
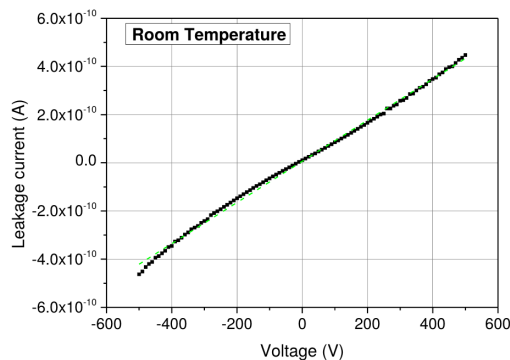


**Figure 9.** Peak centroid and FWHM versus temperature for the 100  $\mu\text{m}$  thick diamond detector with Cr-Cr contacts.

### 5.1.3 Tungsten contacts on 500 $\mu\text{m}$ thick diamond plate

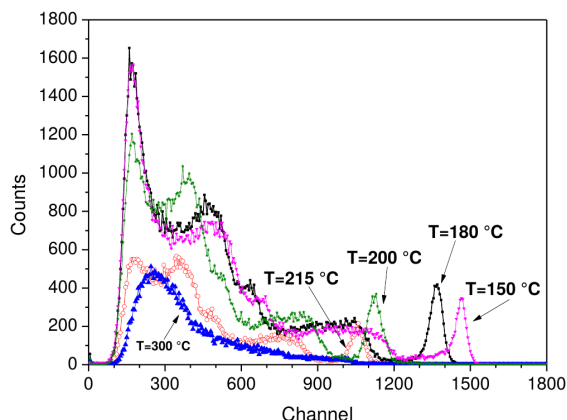
As an example of ohmic metal contacts formed by the annealing procedure we report the results for a diamond detector realized by depositing tungsten contacts on both sides of the film, which were successively annealed at 500°C per 30 minutes so forming *tungsten carbide* (WC). Figure 10 shows the I-V measured at room temperature. An almost linear behaviour can be observed, which is a clear indication of ohmic contact formation.

Figure 11 shows the PHS curves for the detector with WC contacts recorded versus temperature (HV=400 V) by using the digitizer. Also in this case we observed the shift of the peak centroid with the increase of temperature. This detector was not performing very well, and its maximum stable working temperature was  $< 210^\circ\text{C}$  (the lowest achieved in our work), therefore resulting different



**Figure 10.** I-V characteristic for the 500  $\mu\text{m}$  thick diamond with two WC contacts, measured at room temperature after annealing at  $T=500^\circ\text{C}$ . The typical ohmic response is exhibited. The green line is the linear fit; a R-square parameter equal to 0.997 was calculated.

from the findings by other detectors equipped with ohmic contacts, which were well performing till 230–240 $^\circ\text{C}$  [11]. However, as for the other studied detectors, for a constant temperature the detector response was stable, not showing any significant polarization effect. This is shown in figure 12, which reports the data collected at 200 $^\circ\text{C}$  by the digitizer.



**Figure 11.** PHS recorded for the 500 mm thick diamond detector with two tungsten-carbide (WC) contacts, post deposition annealed at 500 $^\circ\text{C}$  per 30 min.

## 5.2 Schottky-ohmic configuration

In the attempt to improve the results, a different type of diamond detector was realized and tested. This detector was made of an intrinsic layer of diamond (i.e. the purchased electronic grade diamond plate) sandwiched between a metal (Schottky) contact and a thin layer (1–3 micron) of diamond highly doped with boron, deposited at Rome “Tor Vergata” University, thus forming an ohmic contact. In the following such a structure will be called “layered detector” or “Schottky-ohmic” detector. The physical characteristics of this type of detector at room temperature are discussed in detail in [21]. However, no attempt was so far reported to investigate its behaviour at high temperature, while irradiated with 14 MeV neutrons. This was done in the present work and the results are reported hereafter.

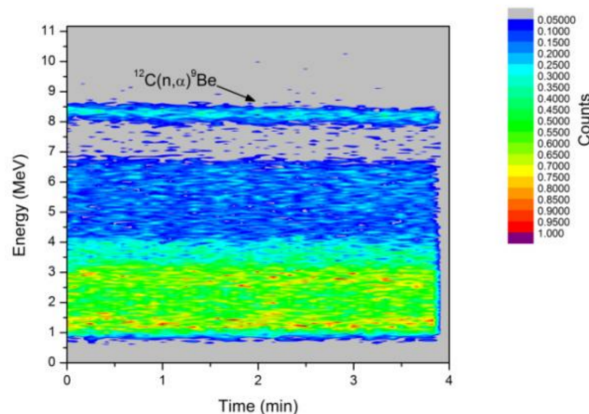


**Figure 12.** Temporal distribution of the pulse height at  $T = 200^\circ\text{C}$  for the 500  $\mu\text{m}$  thick detector with WC contacts.

### 5.2.1 Detector fabrication and characterization

The layered detector was fabricated at ‘Tor Vergata’ University in Rome using a commercial 100  $\mu\text{m}$  thick “electronic grade” CVD single crystal diamond film (dimension  $4,3 \times 4,4 \times 0,1 \text{ mm}^3$ ) purchased by *Micron Electronics* as a substrate. The commercial diamond film was first annealed for 1 h at  $500^\circ\text{C}$  in Argon atmosphere. The layered diamond detector was fabricated by a two steps deposition process. The conductive boron doped diamond homoepitaxial layer, used as backing contact, was deposited by CVD method on the commercial synthetic SCD substrate. The boron layer was about 3  $\mu\text{m}$  thick; its boron concentration was estimated to be about  $0.5 \times 10^{20} \text{ cm}^{-3}$  and its *sheet resistance* was about  $1.5 \text{ k}\Omega/\square$ . After the CVD growth procedure, the diamond layer was oxidized by isothermal annealing at  $500^\circ\text{C}$ , for 1 h in air, in order to remove the conductivity of the as-grown hydrogenated diamond surface. Finally, a circular Cr metal electrode, about 3 mm in diameter and 50 nm in thickness, was deposited on the diamond surface by thermal evaporation. The so fabricated diamond detector was then installed in the detector lay-out discussed in section 2. The detector was operated in reverse bias mode, i.e. with a positive voltage on the top metal contact while the boron doped contact was grounded. The H.V. was  $0.7 \text{ V}/\mu\text{m}$ .

The layered detector was using Cr as metal (Schottky) contact on the second surface because in our experience chromium resulted to be one of the best performing metals for high temperature application. Cr features some important advantages with respect to other metals: high melting point, very good adhesion on diamond surface and it is oxidation resistant. Beside this, according to our tests, Cr features also long lasting operation capability.

It is worth to mention that the presence of a built-in potential of about 1.3 eV due to the Cr Schottky metal/diamond junction allows the detector to be operated without any applied external bias [21]. The layout of the detector is shown in figure 13.

The I-V characteristics were first measured. The typical I-V curve of a diode structure was observed (figure 14). In reverse bias mode the measured current was of the order  $10^{-14} \text{ A}$  while in the forward bias mode the current reached about 1.9 mA at 50 V.

The layered detector was also tested by irradiation with 5.5 MeV alpha particles from  $^{241}\text{Am}$  source. The tests were performed in vacuum and at different bias voltages (reverse bias mode). The

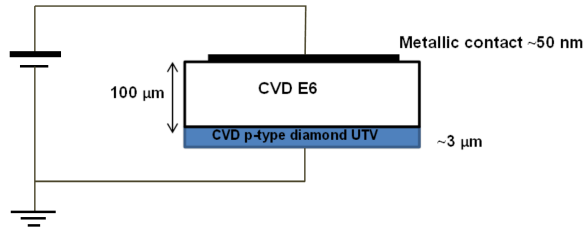


**Figure 13.** Lay-out of the “layered detector”.

readout electronics was composed by a charge preamplifier (ORTEC 142A), a shaping amplifier (ORTEC 570) with  $2 \mu\text{s}$  shaping time and a multi-channel analyser (MCA). The measurement was performed irradiating first the detector from the side of the Cr metal contact and then from the side of the boron contact. The measured PHS are shown in figure 15a and 15b, respectively.

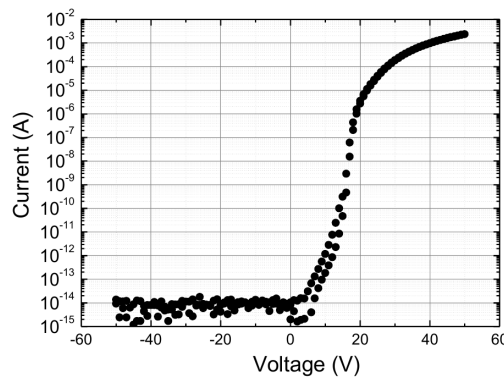


**Figure 14.** Measured I-V characteristic for the  $100 \mu\text{m}$  thick layered detector used in the present work.

As shown in figure 15a, the PHS recorded when the detector is irradiated from the side of the metal-Cr contact presents sharp structure and the peak produced by 5.5 MeV alphas is almost unchanged regardless of the applied bias voltage. Even without any external bias the peak is clearly visible, however it results much more wide thus showing an obvious poorer energy resolution.

When the detector is irradiated from the side of the boron contact the situation is worse (figure 15b), with the peak position shifted toward lower channel values with respect to figure 15a. This is due to the fact that the alphas lose a not negligible fraction of their energy while crossing the  $3 \mu\text{m}$  of the highly borated diamond layer (which is not an active medium for detection), therefore reducing the energy released in the intrinsic diamond layer if compared to the first case in figure 15a. For 5.5 MeV alpha particles, calculation performed with the SRIM code [26] demonstrated that their range in diamond is of the order of  $13.5 \mu\text{m}$ , so in the  $3 \mu\text{m}$  thick borated diamond layer the energy lost by the alphas is about 0.85 MeV. This implies a residual energy of about 4.65 MeV of the alphas entering the detector sensitive volume. Furthermore, the presence of the dead borated diamond layer is further evidenced at very low biasing voltage (5 V) as well as when no bias ( $V = 0 \text{ V}$ ) is applied. Figure 16a and 16b summarize the data reported in figure 15, showing the charge collection efficiency (left axis) and the energy resolution at FWHM (right axis) of the detector as a function of the applied bias voltage. Figure 16a refers to the detector irradiated from the side of the

metallic-Cr contact, while figure 16b shows the same data for the detector irradiated from the side of the boron-doped layer. To note the excellent energy resolution, around 1%, in figure 15a. Again the difference between the two cases is large, especially for the energy resolution (FWHM).

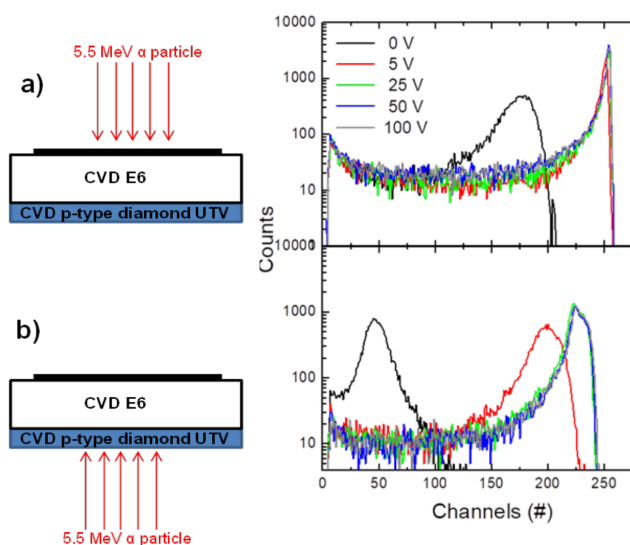


**Figure 15.** Results for the SCD layered detector irradiated with 5.5 MeV alphas from  $^{241}\text{Am}$  a) from the side of the metallic (Cr) contact, and b) from the side of the  $3\ \mu\text{m}$  thick p-type diamond layer.

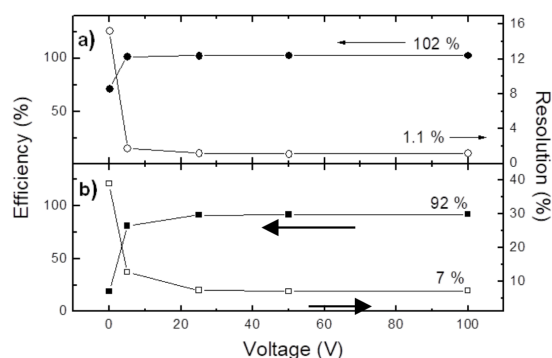
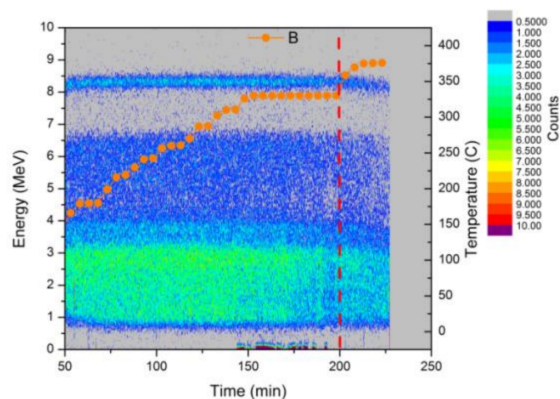


**Figure 16.** Detection efficiency and energy resolution at FWHM for the layered detector irradiated with 5.5 MeV alphas from  $^{241}\text{Am}$ : a) from the side of the metal (Cr) contact, and b) from the side of the  $3\ \mu\text{m}$  thick p-type SCD layer.

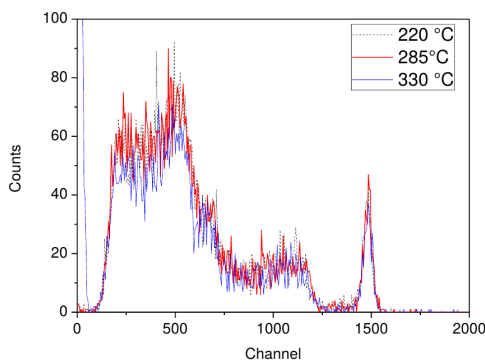
### 5.2.2 Results for the $100\ \mu\text{m}$ thick layered detector under neutron irradiation

Figure 17 reports the time dependent response of the detector under 14 MeV neutron irradiation, i.e. the pulse height versus time as recorded by the digitizer in the temperature range  $220\text{--}375^\circ\text{C}$ . The detector was operated at  $0.7\ \text{V}/\mu\text{m}$  bias voltage. The curve showing the temperature increase is also reported (full orange symbols, right axis). As it can be seen the detector response is almost unaffected by the temperature increase up to about  $330^\circ\text{C}$ , above which a degradation in the detector performance was observed (i.e., a lowering of the pulse height with further temperature increase). For  $T > 400^\circ\text{C}$  the signal was too low to allow for the separation of the  $^{12}\text{C}(n, \alpha)^9\text{Be}$  peak from

the continuous and the measurements were stopped. The plot of some recorded PHS is displayed in figure 18. The excellent stability of the  $^{12}\text{C}(n, \alpha)^9\text{Be}$  peak up to about  $330^\circ\text{C}$  is well evidenced. Again, after cooling the system below the “critical” temperature of  $330^\circ\text{C}$ , the detector properties were restored and it started to operate properly again, thus demonstrating a not destructive effect of the temperature. Figure 19a shows the good stability of the detector during the operation at  $T = 330^\circ\text{C}$ , the irradiation was lasting about 45 minutes. Figure 19b shows the corresponding PHS acquired over the whole 45 minutes measurement time.



**Figure 17.** Time dependent behaviour of the  $^{12}\text{C}(n, \alpha)^9\text{Be}$  peak (top line) recorded during the temperature increase from  $220$  to  $375^\circ\text{C}$ .



**Figure 18.** PHS recorded at increasing temperatures, during irradiation with  $14\text{ MeV}$  neutrons. To note the excellent stability of the measured PHS.

Last, but not least, figure 20 shows the behaviour for the peak centroid and FWHM measured in the whole investigated temperature range.

### 5.2.3 Layered detector $500\ \mu\text{m}$ thick

Owing to the excellent results obtained with the  $100\ \mu\text{m}$  thick B-Cr detector, a second layered detector was fabricated using a  $500\ \mu\text{m}$  thick diamond plate. The deposition procedure for both contacts was as discussed above. The  $500\ \mu\text{m}$  thick diamond was operated with  $0.7\ \text{V}/\mu\text{m}$ . The electronic chain was the same as before. The detector was thus irradiated with  $14.1\ \text{MeV}$  neutrons

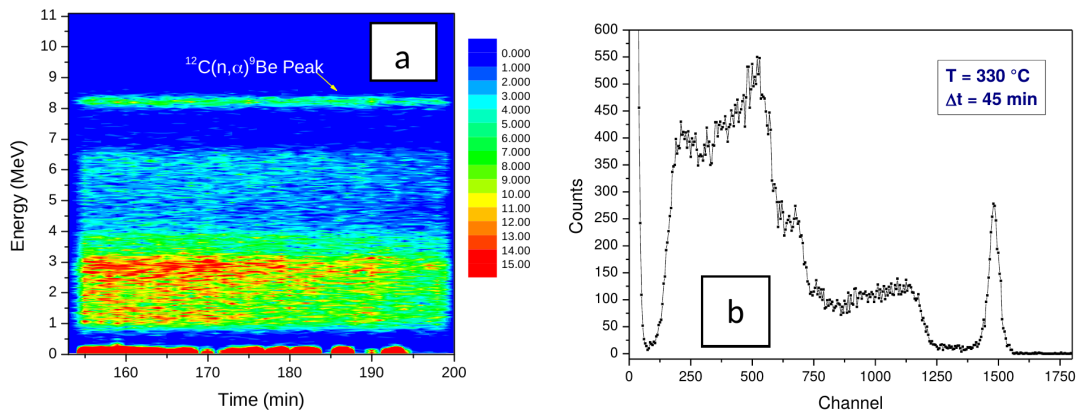


**Figure 19.** a) Pulse height recorded with the digitizer during 45 minutes lasting irradiation at  $T=330^\circ\text{C}$ ; b) The PHS recorded during the 45 minutes lasting irradiation at  $T= 330^\circ\text{C}$ .

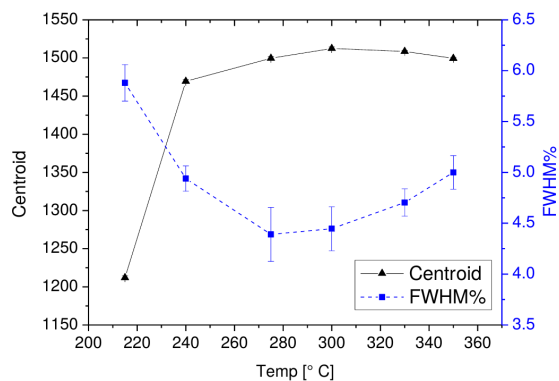


**Figure 20.** Peak centroid (right) and peak FWHM (left) versus temperature for the  $100\ \mu\text{m}$  B-Cr detector.

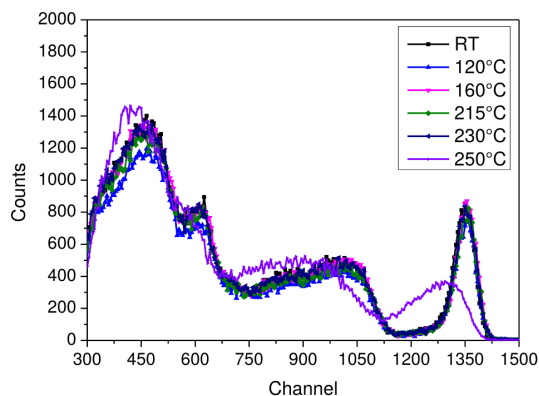


**Figure 21.** PHS as function of the temperature for the  $500\ \mu\text{m}$  thick B- Cr detector.

and the PHS recorded as function of the temperature. In figures 21 and 22 the recorded PHS, the peak centroid and the FWHM are reported versus temperature.

As shown in figures 21 and 22, the detector exhibited a good energy resolution ( $<5\%$  at FWHM) up to  $\sim 230^\circ\text{C}$ , however its maximum working temperature was about  $230^\circ\text{C}$ , much lower

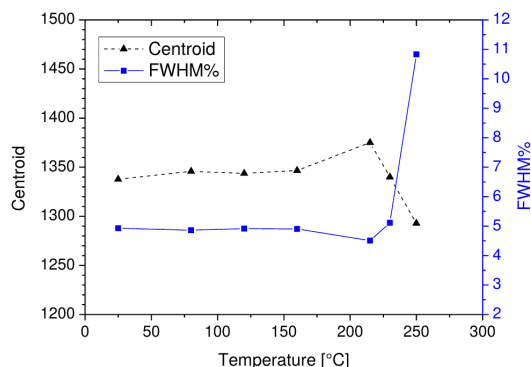


**Figure 22.** Energy resolution and  $^{12}\text{C}(n, \alpha)^9\text{Be}$  peak centroid position as function of the temperature for the 500  $\mu\text{m}$  thick B-Cr detector.

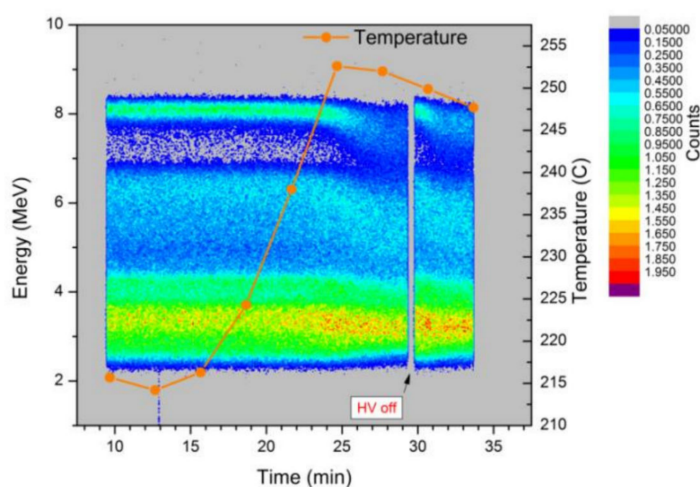


**Figure 23.** Measured pulse height temporal distribution as function of the temperature for the 500  $\mu\text{m}$  thick layered detector. The red curve is the temperature vs. time (right axis).

than that previously reported for the 100  $\mu\text{m}$  thick layered detector. In figure 23 the time stability of the detector, as measured by the digitizer, is shown. This confirms the results reported above.

As it is possible to see in figure 23, the events related to the  $^{12}\text{C}(n, \alpha)^9\text{Be}$  peak are located at about 8.5 MeV. At about  $\sim 235^\circ\text{C}$ , the  $^{12}\text{C}(n, \alpha)^9\text{Be}$  peak sharply drops toward lower energy values. Furthermore, figure 23 also shows that for  $T > 240^\circ\text{C}$ , by switching ON/OFF the HV the performance of the detector is re-established for a very short time before a new loss in detection capabilities. This phenomenon is reasonably consistent with the presence of polarization effects.

A common feature shared by the two studied layered detectors is the good stability of the peak centroid as temperature increases up to the maximum operational limit, above which, also for the layered detectors, we observed the shift of the peak centroid toward lower energy. This was not observed with the other studied detectors reported in this work, except for the Ag annealed contacts, as reported in [11].

## 6 Discussion

The finding of this work (just a selection among the available results are reported in this paper) is that the type and the quality of the fabricated electrical contacts slightly affect the response of the detector, both in term of maximum working temperature and detector performance (e.g. energy resolution). Owing to our results,  $T \sim 220^\circ\text{C}$  can be considered as “safe” operational temperature limit, regardless of the type of electrical contact. Therefore, according to our data, the impact of the contact-type can impact on the above maximum working temperature within a range of  $-5^\circ\text{C}$  (lower limit  $215^\circ\text{C}$ ) and  $+15^\circ\text{C}$  (upper limit  $235^\circ\text{C}$ ). The only exception, toward higher temperature, being the  $100\ \mu\text{m}$  thick layered detector.

Above  $230\text{--}240^\circ\text{C}$  the behaviour of the detector seems to be affected by “polarization” The latter is due to the build-up of space charge inside the detector which in turn produce a locally reduced electrical field (to note that the trapping probability of charge carriers is proportional to the thickness of the collecting region). This causes an increase in charge carriers recombination (both electrons and holes) which lead to a reduced charge collection efficiency. In our measurement the latter was evidenced by the shifting of the  $^{12}\text{C}(n, \alpha)^9\text{Be}$  peak toward lower energy in the pulse eight spectra (PHS). Polarization compromises quickly the detector performance and the overall detection capabilities. An interesting aspect is that once cooled down ( $T < 200\text{--}210^\circ\text{C}$ ) the detector performances are restored and this was observed also by cycling the temperature (heating followed by cooling) of the detectors. This is indicating that the operation at high temperature does not damage the detector and that the observed detrimental phenomena are probably to be ascribed to intrinsic thermal properties of diamond such as the presence of some deep trap levels which activate for  $T > 220\text{--}230^\circ\text{C}$ . The latter point was already reported by other authors in [27, 28] where there is report about the presence of deep traps in diamonds with activation energy  $>1\ \text{eV}$ . The reported activation levels are compatible with the maximum temperature achieved. In [27] it is suggested that the observed traps with their high capture rate (carrier recombination), which depends on the trap concentration, can be effective in limiting carrier lifetime and thus charge collection distance (CCD). We point out that the observed polarization behaviour has several similarities with what is observed for radiation damaged diamond detectors [29]. In this case the polarization is originated by traps formed by the radiation.

Another result of the present study is the evidence of a possible dependence of the working temperature from the diamond film thickness. Our results show that the thinnest detectors ( $100\ \mu\text{m}$ ) exhibit the highest working temperature (e.g.  $\sim 270^\circ\text{C}$  for the Cr-Cr contacts) while keeping very good performances. In one case, for the  $100\ \mu\text{m}$  thick detector with B-Cr contacts we got a temperature limit of  $\sim 330^\circ\text{C}$ , however, we stress once more that this result was never replicated. To clarify this point new measurements with much more thin detectors (e.g.  $25\text{--}50\ \mu\text{m}$ ) should be performed, the problem is that they are not available on the market. Concerning the effect of the film thickness, it worth to mention that in eq. (8) of ref. [30] it is demonstrated that the thickness of the diamond film affects the current produced under irradiation, the thinner the detector the higher the current.

Our results are substantially in agreement with the data reported in [10], however we want to stress once more a fundamental difference between our work and reference [10]. While the measurements in [10] were performed under vacuum condition using alphas particles (at low

emission rate) and a detector design not suited for being located in a real harsh environment, the present work was performed using the prototype of a detector designed for to be hosted in harsh environment. The measurements were performed in air and this is another point to be considered since the effect of secondary electrons and of air ionization cannot be excluded, especially for detectors operating under intense radiation field. Moreover, all the results indicate that the presence e.g. of mineral cable and MOC does not affect the response of the detector when compared to the results in [10]. This is a further indication that the main reason for the observed operational temperature limit is to be ascribed to intrinsic properties of diamond. To complete this discussion, it is worth to point out that in some cases, e.g. with annealed Ag contacts [11] or with the layered detectors with B-Cr contacts (the latter both for 100 and 500  $\mu\text{m}$  thick detectors), the peak position is stable with the temperature increase up to the rise of the polarization effect. The question is whether this behaviour could be ascribed to the used electrical contacts. Indeed, the electrical contact can affect the charge collection rate by which the carriers are collected and removed. Different metals and/or different deposition/post-deposition procedures can alter in a different way the interface between the electrical contact (e.g. metal) and the diamond film so producing defects (interface defects) with different characteristics (e.g. activation energies, cross section, etc.) respect to those already available in the diamond film (intrinsic defects). These defects could, in turn, affect the carriers dynamics and collection especially under the effect of temperature. If these defects have activation energies lower than the that of the intrinsic defects they activate at lower temperatures and thus we can expect polarization effects to start at lower temperatures and we observe the peak shifting. Viceversa, if these defects have higher activation energy than the intrinsic defects they do not activate and the detector behaviour is stable up to the intrinsic defects activate.

## 7 Conclusions

A systematic study of the response, at variable temperature, of artificial single crystal diamond detectors produced by using commercial diamond film and equipped with different types of electrical contacts and irradiated with 14 MeV neutrons was performed.

Three types of electric contacts produced both using metal and not metal layers were investigated: *a)* double Schottky, *b)* double ohmic; *c)* Schottky-ohmic contacts. The detectors were operated in pulse mode. The pulse height spectra produced by 14 MeV neutron irradiations were recorded as a function of temperature. The detector behaviour was studied by analysing versus temperature the parameters of the peak produced in the PHS by the  $^{12}\text{C}(n, \alpha)^9\text{Be}$  reaction induced by 14 MeV neutrons in carbon (peak position, FWHM, peak area).

The maximum operational temperature limit of the tested detectors was found to be around 230°C and it resulted to be slightly dependent, within  $\pm 10^\circ\text{C}$ , upon the type of the electrical contact. It turned out that, together with the type of the electrical contact, other parameters such as the intrinsic diamond proprieties (e.g. deep traps) and the film thickness have to be considered to understand the response of the detector at high temperature. The effect of the films thickness call for further investigation using diamond films more thinner than those used in this work (e.g.  $< 50 \mu\text{m}$ ). As the used diamond films were all from the same producer this work calls for the need to investigate also diamond films from different producers so to point out whether the reported operational temperature limit is to be ascribed to the intrinsic properties (e.g. impurities) of the used diamond films.

## Acknowledgments

The work leading to this publication was partly supported by F4E under the Specific Grant Agreement F4E-FPA-395-01 and 02. The views and opinions expressed herein do not necessarily reflect those of F4E.

## References

- [1] A. Paoletti and A. Tucciarones, *The Physics of diamond*, in proceedings of the *International School of Physics “E. Fermi”*. Course CXXXV, Varenna, Italy, 23 July–2 August 1996, IOS Press (1997).
- [2] S. Koizumi, C.E. Nebel and M. Nesladek, *Physics and Application of CVD Diamond*, WILEY-VCH Verlag GmbH Co. KGaA, Weinheim Germany (2008) [ISBN: 978-3-527-40801-6].
- [3] M. Angelone et al., *Single crystal artificial diamond detectors for VUV and soft X-rays measurements on JET thermonuclear fusion plasma*, *Nucl. Instrum. Meth. A* **623** (2010) 726.
- [4] M. Pillon et al., *Development of on-line tritium monitor based upon artificial diamond for fusion applications* *IEEE Trans. Nucl. Sci.* **58** (2011) 1141.
- [5] M. Pillon et al., *Diamond based neutron spectrometer for diagnostics of deuterium-tritium fusion plasmas*, in proceedings of the *21st IEEE/NPS Symposium on Fusion Engineering SOFE 05*, Knoxville, TN, U.S.A., 26–29 September 2005, pp. 1–4.
- [6] L. Bertalot et al., *ITER relevant developments in neutron diagnostics during the JET trace tritium campaign*, *Fusion Eng. Des.* **74** (2005) 835.
- [7] D. Leichtle et al., *The F4E programme on nuclear data validation and nuclear instrumentation techniques for TBM in ITER*, *Fusion Eng. Des.* **89** (2014) 2169.
- [8] M. Angelone et al., *Neutronics experiments, radiation detectors and nuclear techniques development in the EU in support of the TBM design for ITER*, *Fusion Eng. Des.* **96–97** (2015) 2.
- [9] M. Angelone et al., *Spectrometric performances of monocrystalline artificial diamond detectors operated at high temperature*, *IEEE Trans. Nucl. Sci.* **59** (2012) 2416.
- [10] A. Metcalfe, G.R. Fern, P.R. Hobson, D.R. Smith, G. Lefeuvre and R. Saenger, *Diamond based detectors for high temperature, high radiation environments*, in proceedings of the *18th International Workshop on Radiation Imaging Detectors (iWoRiD 2016)*, Barcelona, Spain, 3–7 July 2016, [2017 JINST 12 C01066](#).
- [11] R. Pilotti et al., *Development and high temperature testing by 14 MeV neutron irradiation of single crystal diamond detectors*, [2016 JINST 11 C06008](#).
- [12] <https://www.e6.com>.
- [13] M. Martone, M. Angelone and M. Pillon, *The 14 MeV Frascati neutron generator*, *J. Nucl. Mater.* **212–215** (1994) 1661.
- [14] R.T. Tung, *The physics and chemistry of Schottky barrier height*, *Appl. Phys. Rev.* **1** (2014) 011304.
- [15] N. Tatsumi, K. Ikeda, H. Umezawa and S.-i. Shikata, *Development of diamond schottky barrier diode*, *SEI Tech. Rev.* **68** (2009) 54.
- [16] T. Teraji, Y. Koide and T. Ito, *Schottky barrier height and thermal stability of p-diamond (100) schottky interfaces*, *Thin Solid Films* **557** (2014) 241.
- [17] M. Werner, *Diamond metallization for device applications*, *Semicond. Sci. Technol.* **18** (2003) S41.

- [18] J.C. Rivière, *Solid State Surface Science. Volume 1*, M. Green ed., Marcel Dekker, New York U.S.A. (1969).
- [19] J. Hölzl, F.K. Schulte and H. Wagner, *Solid Surface Physics*, Springer Tracts in Modern Physics, volume 85, Springer-Verlag (1979).
- [20] S. Almaguer et al., *Chemical vapor deposition diamond based multilayered radiation detector: Physical analysis of detection properties*, *J. Appl. Phys.* **107** (2010) 014511.
- [21] A. Balducci et al., *Extreme ultraviolet single-crystal diamond detectors by chemical vapor deposition*, *Appl. Phys. Lett.* **86** (2005) 193509.
- [22] I. Ciancaglioni et al., *Influence of the metallic contact in extreme-ultraviolet and soft X-ray diamond based schottky photodiodes*, *J. Appl. Phys.* **110** (2011) 054513.
- [23] M. Pillon, M. Angelone, A. Krása, A. Plompen, P. Schillebeeckx and M. Sergi, *Experimental response functions of a single-crystal diamond detector for 5–20.5 MeV neutrons*, *Nucl. Instrum. Meth. A* **640** (2011) 185.
- [24] M. Angelone et al., *Development of single crystal diamond neutron detectors and test at JET tokamak*, *Nucl. Instrum. Meth. A* **595** (2008) 616.
- [25] M. Angelone et al., *Time dependent 14 MeV neutrons measurement using a polycrystalline chemical vapor deposited diamond detector at the JET tokamak*, *Rev. Sci. Instrum.* **76** (2005) 013506.
- [26] <http://www.srim.org>.
- [27] M. Bruzzi, D. Menichelli, S. Sciortino and L. Lombardi, *Deep levels and trapping mechanisms in chemical vapor deposited diamond*, *J. Appl. Phys.* **91** (2002) 5765.
- [28] P. Bergonzo et al., *Improving diamond detectors: A device case*, *Diamond Relat. Mater.* **16** (2007) 1038.
- [29] F. Kassel, M. Guthoff, A. Dabrowski and W. de Boer, *Severe signal loss in diamond beam loss monitors in high particle rate environments by charge trapping in radiation-induced defects*, *Phys. Status Solidi A* **213** (2016) 2641 [[arXiv:1609.07949](https://arxiv.org/abs/1609.07949)].
- [30] M. Angelone, S. Cesaroni, S. Loreti, G. Pagano and M. Pillon, *High temperature response of a single crystal CVD diamond detector operated in current mode*, *Nucl. Instrum. Meth. A* **943** (2019) 162493.